Transient 2D IR spectroscopy from micro- to milliseconds

Hamm, Peter

Abstract: A new application of high-repetition rate, femtosecond Yb-laser/amplifier systems is introduced: transient 2D IR spectroscopy covering the time range from micro- to milliseconds. This approach intertwines the measurement of 2D IR spectra with the time separation from an actinic pump pulse and utilizes the high repetition rate of these lasers systems in two ways: by offering a high time resolution (10 µs) and by enabling the measurement of many 2D IR spectra. The well-studied photocycle of bacteriorhodopsin is used as a demonstration object in this proof-of-principle experiment.

DOI: https://doi.org/10.1063/5.0045294

The Journal of Chemical Physics ARTICLE scitation.org/journal/jcp

Transient 2D IR spectroscopy from micro- to milliseconds

Cite as: J. Chem. Phys. 154, 104201 (2021); doi: 10.1063/5.0045294
Submitted: 25 January 2021 • Accepted: 22 February 2021 •
Published Online: 11 March 2021

Peter Hamm[a)]

AFFILIATIONS

Department of Chemistry, University of Zurich, Winterthurerstr. 190, CH-8057 Zürich, Switzerland

Note: This paper is part of the JCP Special Topic on Coherent Multidimensional Spectroscopy.
[a)]**Author to whom correspondence should be addressed:** peter.hamm@chem.uzh.ch

ABSTRACT

A new application of high-repetition rate, femtosecond Yb-laser/amplifier systems is introduced: transient 2D IR spectroscopy covering the time range from micro- to milliseconds. This approach intertwines the measurement of 2D IR spectra with the time separation from an actinic pump pulse and utilizes the high repetition rate of these lasers systems in two ways: by offering a high time resolution (10 μs) and by enabling the measurement of many 2D IR spectra. The well-studied photocycle of bacteriorhodopsin is used as a demonstration object in this proof-of-principle experiment.

I. INTRODUCTION

Diode-pumped Yb-lasers/amplifiers with high average powers and high repetition frequencies of $\gtrsim$100 kHz are an emerging technology in femtosecond sciences.[1–3] Their fundamental wavelength around 1030 nm is farther in the IR than that of Ti:S laser systems, making them, in particular, interesting for mid-IR generation, since this wavelength regime can be reached in a single frequency conversion step with lithium gallium sulfide (LGS) crystals.[4] Multidimensional spectroscopy in the IR range (2D IR) is a powerful tool to study the structure and dynamics of solution phase molecular systems,[5–10] but the sensitivity is often an issue when samples with small concentrations or IR vibrations with small cross sections are considered.[11] Besides their excellent inherent stability, the high repetition frequencies of Yb lasers/amplifiers should also improve the sensitivity by averaging more data within a given measurement time. However, the number of publications, which report on 2D IR instruments based on such Yb lasers/amplifiers, is still rather limited.[12–20] The motivation of these works is either higher sensitivity[16,19] or collecting many 2D IR spectra, e.g., in the context of 2D IR microscopy[17] or high-throughput applications.[15,18]

Here, another application of the high repetition rates of these lasers is introduced: transient 2D IR spectroscopy. The idea to use such lasers for transient IR spectroscopy (which will be called transient 1D IR spectroscopy in the following) has been demonstrated before,[21] where an actinic pump pulse triggers a photo-reaction and a sequence of IR probe pulses, separated by 10 μs (i.e., 100 kHz), measures the one-dimensional transient IR response from a few microseconds to, in principle, infinity. In transient 2D IR spectroscopy, the sequence of three IR pulses (i.e., a pair of two IR pump pulses and an IR probe pulse) measures a 2D IR spectrum at a given delay time τ_a after the actinic pump pulse [Fig. 1(a)]. The first demonstration of transient 2D IR spectroscopy generated all pulses, the actinic pump pulse and IR pump and probe pulses, from one laser and used conventional optical delay stages to generate the required pulse sequence.[22–25] Each IR pulse sequence needed to construct the 2D IR spectrum, scanning the IR pump pulses, had its own preceding actinic pump. The time resolution of this type of experiment is in the range of a few picoseconds, i.e., the scan range τ_{2D} between the two IR pump pulses, while the maximum time delay τ_a is limited by the travel range of optical delay stages, typically a few nanoseconds. When deriving actinic pump and IR pulses from two laser systems whose relative timing is either controlled or measured,[26–28] the maximum time delay would ultimately be limited by the repetition rate of the laser, i.e., the time when the next actinic pump pulse arrives at the sample (10 μs for a 100 kHz laser). Zanni and co-workers, in contrast, promoted "rapid-scan" 2D IR spectroscopy,[29,30] making use of acousto-optic pulse shapers,[31] which allows for a shot-by-shot modulation of the IR pump-pulse pair. A complete 2D IR spectrum can be measured with typically a few

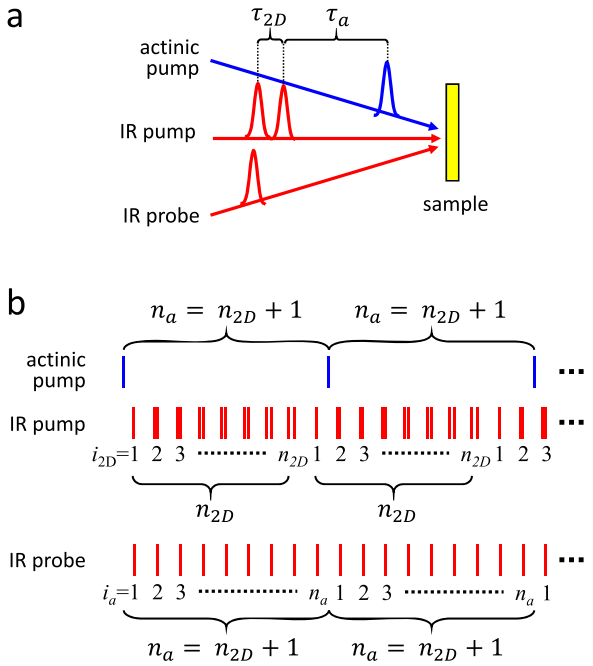

FIG. 1. (a) Basic pulse sequence of transient 2D IR spectroscopy. (b) Repetitive pulse sequence used here to measure a sequence of transient 2D IR spectra. IR probe pulses (bottom row) are generated at a repetition rate of 100 kHz (Δt = 10 μs), together with a pair of IR pump pulses (middle row) produced with the help of a pulse shaper on a single shot basis. In total, n_{2D} IR laser shots are needed to construct one 2D IR spectrum. The actinic pump (top row) has a periodicity of $n_a = m \times n_{2D} + 1$ with any integer number m (m = 1 is shown here).

100 laser shots, i.e., a few milliseconds for a 100 kHz laser, determining the time resolution of this type of experiment.

II. CONCEPT

The approach presented here bridges the gap between these two extremes, intertwining the measurement of the 2D IR spectrum with the time separation from the actinic pump pulse. Timescales τ_a from a few microseconds to tens of milliseconds can be covered in this way. Figure 1(b) illustrates the basic idea. IR probe pulses are generated at a 100 kHz repetition rate by an Yb-laser system. IR pump pulse pairs are generated with the help of a pulse shaper on a single shot basis,[30,31] collecting the data for a full 2D IR spectrum with n_{2D} IR laser shots. While Fig. 1(b) shows that the various pulse shaper states control only the time separation between the two pump pulses, additional pulse shaper states are introduced in reality for phase cycling. Note also that the scheme of Fig. 1(b) is not on scale regarding time as the time separation between subsequent IR probe pulses is 10 μs, while that between the two IR pump pulses is in the range of a few picoseconds only.

The periodicity of the actinic pump pulses is offset by one laser pulse,

$$n_a = m \cdot n_{2D} + 1, \quad (1)$$

with any integer number m [Fig. 1(b) shows m = 1]. Due to that offset of 1, all pulse shaper states are obtained for each delay time after the actinic pump after collecting $n_a \times n_{2D}$ laser pulses. For example, the first IR pulse sequence after the first actinic pump shown in Fig. 1 is for (i_a = 1, i_{2D} = 1), that after the second actinic pump pulse is for (i_a = 1, i_{2D} = 2), and that after the third actinic pump is for (i_a = 1, i_{2D} = 3). The second IR pulse sequences after each actinic pump pulse are for (i_a = 2, i_{2D} = 2), (i_a = 2, i_{2D} = 3), and (i_a = 2, i_{2D} = 4), and so on. After properly resorting the data, one can construct a sequence of n_a 2D IR spectra separated by 10 μs each. With the help of m in Eq. (1), one can choose the maximum delay time τ_a after the actinic pump essentially independent of the number n_{2D} of laser shots needed to construct a 2D spectrum.

The sample chosen for this proof-of-principle experiment is bacteriorhodopsin,[32] an extremely well-studied photo-active protein,[33,34] which is very stable and undergoes a fast photocycle.[33,35,36] It is a light driven proton pump consisting of an α-helical *trans*-membrane protein with a retinal molecule bound to Lys216 via a Schiff base. Photo-excitation induces the *trans*-to-*cis* isomerization of the chromophore around one of its C=C double bonds on a 500 fs timescale.[37] It then circles through a sequence of intermediates commonly denoted as J to O (where the M-intermediate is assumed to be split into two states M_1 and M_2, which are spectroscopically very similar). The Schiff base is deprotonated during the L–M_1 transition, and the proton is transferred to Asp85. It is then reprotonated from Asp96 during the M_2—N transition. Thermal back-isomerization of the chromophore occurs during the N—O transition, and deprotonation of Asp85 completes the catalytic cycle.[33] We have performed transient 2D IR experiments of bacteriorhodopsin on a picosecond timescale before,[24] looking at the first J-intermediate of the photocycle. The time window of the present experiment will cover the L, M, N, and O intermediates, while the K-intermediate is mostly decayed by the time the present experiments starts.

III. METHODS

For the IR pulses, the output of an Yb-doped fiber laser/amplifier system (short-pulse Tangerine, Amplitude, France) with a central wavelength of 1035 nm, pulse energy of 200 μJ, pulse duration of 150 fs, and repetition rate of 100 kHZ was used to pump an optical parametric amplifier (OPA) (Twin STARZZ, Fastlite, France) with a subsequent frequency mixing stage in a LGS crystal. The typical bandwidth of the IR pulses is 100–150 cm^{-1}, and a pulse energy of 0.9 μJ has been used to minimize thermal effects in the sample. With the help of a BaF_2 wedge, the IR pulses were split into IR pump, probe, and reference pulses. Probe and reference pulses were focused into the sample (spot size: 100 μm) slightly offset, transmitted through a spectrograph, and detected with the help of a 2 × 32-MCT detector array with a spectral resolution of 3.5 cm^{-1} in the probe direction. The detector signals were amplified and digitized with a custom-designed electronics, as described in Ref. 19. Referencing was optimized using the method described in Ref. 38, making use of the correlation between all pixels of the detector.

The IR pump pulses were sent through a pulse shaper (PhaseTech Spectroscopy) in order to generate a pair of pump pulses with programmable delay times and phases and spatially overlapped with the probe pulses in the sample. Working in a rotating frame, n_{2D} can be optimized down to 164 laser shots with a total scan time of 2 ps in 41 steps (time step 50 fs, spectral resolution in the pump

direction of 8 cm^{-1}) and four phase cycles can be used to suppress scatter. A small number n_{2D} is desirable to keep $n_a \times n_{2D}$ small and thereby increase the amount of averages per 2D IR spectrum. The delay between IR pump and probe pulses in the sample (i.e., the population time) was set to 200 fs with the help of a conventional delay stage in order to avoid artifacts from pump–probe overlap.

Actinic pump pulses at 447 nm were generated with a GaN multimode laser diode (PLPT9 450D_E, Osram Opto Semiconductors) and operated by a pulsed laser diode driver (LDP-V 10-10, PicoLAS) to produce pulses of 2 μs length. While the maximum power of the laser diode is specified at 3.5 W in cw-operation, one can go up to 10 W in pulsed operation, revealing 20 μJ of pulse energy in the 2 μs long pulses. The laser diode beam was pre-collimated (LTN330-C, Thorlabs); its elliptical shape was corrected with two cylindrical lenses (50 and 150 mm) and then focused into the sample with a 100 mm lens, matching the diameter of the IR pulses. All beams (IR pump and probe as well as actinic pump) were polarized in parallel. The timings of all components in the setup have been controlled with a programmable delay generator (T560, Highland Technology). The measurement electronics also read two synchronization signals needed to properly sort the data, one from the actinic pump laser and the second from the pulse shaper.

The period of the actinic pump was set to $n_a = 3445$ (i.e., $m = 21$, repetition rate 29 Hz), determining a maximum delay time τ_a of about 33 ms (2 ms preceding the actinic pump were used for a reference 2D IR spectrum). With these numbers, $n_a \times n_{2D} = 564\,980$, and it takes 5.6 s for one complete dataset. The data shown here were averaged over 13 000 such datasets, which took about 20 h of measurement time. The Yb-laser/OPA system is stable enough to allow for such long measurement times without the need of any readjustments.

Bacteriorhodopsin purple membrane patches were prepared according to standard procedures[39] and were provided by Martin Engelhard (Max Planck Institute for Molecular Physiology). The solvent was exchanged to D_2O at a concentration of ≈2 mM, and the sample was held in a stationary CaF_2 cuvette with 25 μm spacing.

Difference 1D and 2D IR spectra will be shown, which require the subtraction of stationary reference spectra from the transient spectra. This, in turn, requires that the sample completely reaches its ground state before each actinic pump pulse, in which case one can use an average of a certain number (in the present case, 200) of spectra before the actinic pump as a reference spectrum. In that regard, it helps that the photocycle of bacteriorhodopsin completes quickly after 35 ms (this timescale essentially sets the value for n_a), without the need to exchange the pumped sample volume by moving the cuvette or by pumping the sample through the cuvette. Furthermore, bacteriorhodopsin is very stable, surviving many hours of measurement time on the same spot.

IV. EXPERIMENTAL RESULTS

To set the stage, Fig. 2(a) shows transient 1D IR spectra (similar data have been collected before),[40–42] covering the time window from 5 μs to 33 ms and the spectral range of the ethylenic stretch vibration of the retinal chromophore around 1525 cm^{-1}. The transient 1D IR spectra have been measured by blocking the IR pump pulses and setting the timing of the actinic pump in the middle between two IR probe pulses. Data are shown in Fig. 2(a) as obtained up to 100 μs and binned on a logarithmic timescale with 20 time points per decade beyond. The presented excellent data quality is obtained with only 1 min of averaging.

The dominant feature is a negative (blue) bleach of the ethylenic stretch vibration [labeled BR in Fig. 2(a) for the resting state of bacteriorhodopsin], which exists for all intermediates of the photocycle covered by this experiment (K to O intermediate). This mode reveals the strongest difference band in the transient 1D IR spectrum since it is affected directly by photo-isomerization.[43] In the various intermediates of the photocycle, the ethylenic stretch vibration shifts to different frequencies, showing up as positive bands in Fig. 2(a).[42] In the K-intermediate, whose lifetime is ≈2 μs, the band appears at 1510 cm^{-1}, a remainder of which is still visible at very early delay times. The L-intermediate, in turn, exhibits a frequency up-shifted band at 1547 cm^{-1}. The M-intermediate, which peaks at around 300 μs,[35,36] does not have any distinct positive band in this spectral range. The N and O intermediates strongly overlap in

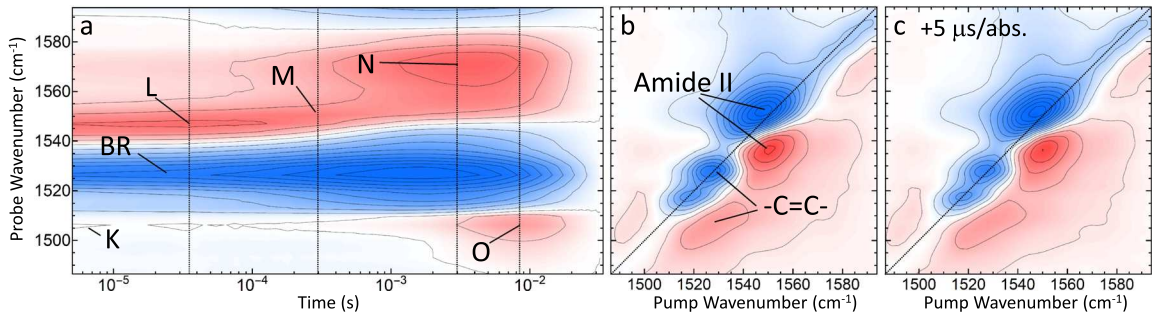

FIG. 2. (a) Transient 1D IR spectra of bacteriorhodopsin as a function of time, showing negative bleach contributions in blue and positive new bands in red. The dashed vertical lines mark the time points when the L, M, N, and O intermediates peak and relate to the delay times shown in Fig. 4. (b) Stationary 2D IR spectrum of light-adapted bacteriorhodopsin in the same frequency range, showing negative bleach contributions in blue and excited state absorption in red. The spectrum has been averaged over the 2D IR spectra starting from −2 ms before the actinic pump pulse (i.e., 200 individual 2D IR spectra). Assignable spectroscopic features are labeled and discussed in the text. (c) Absolute 2D IR spectrum measured 5 μs after the actinic pump.

time[36,42] but have very distinct spectroscopic signatures at 1570 and 1510 cm^{-1}, respectively.

Figure 2(b) shows the stationary 2D IR spectrum of light-adapted bacteriorhodopsin in the same frequency range. In essence, it consists of two bands centered at 1525 and 1550 cm^{-1}, respectively, each of which with the characteristic peak pair of negative ground-state bleach colored in blue and anharmonically red-shifted excited state absorption colored in red.[9] The frequency of the first band (labeled −C=C−) coincides with the dominant bleach in the transient 1D IR data [Fig. 2(a)] and thus is assigned to the ethylenic stretch vibration of the retinal chromophore. The second peak pair originates from the amide II band of the protein backbone. Its 2D IR response is considerably stronger since many more normal modes contribute to it (one per amino acid), but the band is hardly affected by photo-isomerization of the chromophore, and therefore, it does not show up in the transient 1D IR spectrum of Fig. 2(a).

Figure 2(c) shows the 2D IR spectrum measured 5 μs after the actinic pump, which differs from that in Fig. 2(b) in two regards. First, it is much noisy (which is barely visible on the scale of the plot), as it is averaged less. Only 20 s of total measurement time went into this 2D IR spectrum, yet the quality is excellent, illustrating the superior noise properties of the Yb-laser system in combination with single-pulse modulation made possible by using the pulse shaper. The 2D IR spectrum in Fig. 2(b), in contrast, is averaged over 200 such spectra measured before the actinic pump and will be used as a reference spectrum. Second, it is the 2D IR spectrum of a sample with a certain fraction of switched bacteriorhodopsin molecules. However, it is hard to tell the difference between the two 2D IR spectra in Figs. 2(c) and 2(b) since the actinic pump does not excite 100% of the molecules, since the photo-isomerization quantum yield is smaller than 100%, and since the stationary 2D IR spectrum is dominated by the amide II band, which is hardly affected by photo-switching. Therefore, difference 2D IR spectra need to be calculated to distill out the small changes, just like it is common for transient 1D IR spectroscopy [Fig. 2(a)].

Figure 3 exemplifies two such difference spectra, the left one just before the actinic pump at −5 μs and the right one just after the actinic pump at +5 μs. The spectrum at +5 μs is the difference of the 2D IR spectrum shown in Fig. 2(c) and the reference 2D IR spectrum shown in in Fig. 2(b) (the spectrum at −5 μs has been calculated accordingly, but the corresponding absolute spectrum is not shown). The scale of Fig. 3 is magnified by a factor of 10 relative to that of Figs. 2(b) and 2(c). The spectrum at −5 μs reveals the noise level of the experiment, while a clear 2D IR signature is obtained in the spectrum at +5 μs. The signal-to-noise ratio in this spectrum is ≈10:1, implying that the signal-to-noise ratio of the absolute spectrum of Fig. 2(c), whose amplitude is ten times larger, is ≈100:1, within only 20 s of averaging time.

Figure 4 shows a sequence of transient 2D IR spectra at time points chosen to maximize the contributions from the L, M, N, and O intermediates. In order to further improve the signal-to-noise ratio, they have been binned over 3 (35 and 300 μs), 35 (3 ms), and 97 (8.4 ms) individual difference 2D IR spectra of the type shown in Fig. 3, respectively. Such transient 2D IR spectra are double-difference spectra, i.e., the difference between the two 2D IR spectra of the reactant and product, each of which consists of the difference between the ground-state contribution and the anharmonically shifted excited state absorption. In either case, the spectral shifts are often small compared to the linewidth of the spectroscopic transitions, and contributions with opposite signs tend to cancel each other. Furthermore, the partial cancellation of contributions with opposite signs in transient 2D IR spectroscopy is different from that in transient 1D IR spectroscopy since only the former resolves inhomogeneous broadening. A relatively small change in the ratio of homogeneous vs inhomogeneous broadening upon switching from the reactant and product can cover one of them completely in the transient 2D IR spectrum, despite the fact that both show up in the transient 1D IR spectrum. All these aspects can make the interpretation of transient 2D IR spectra cumbersome.[22]

Starting with the dominant bleach of the ethylenic stretch vibration at around 1525 cm^{-1} [Fig. 2(a)], one expects a 2D IR signature with inverted signs in the transient 2D IR spectra since it is the 2D IR response of a bleaching (negative) band. That is, one expects a positive (red) band on the diagonal originating from the ground-state contribution together with a negative (blue)

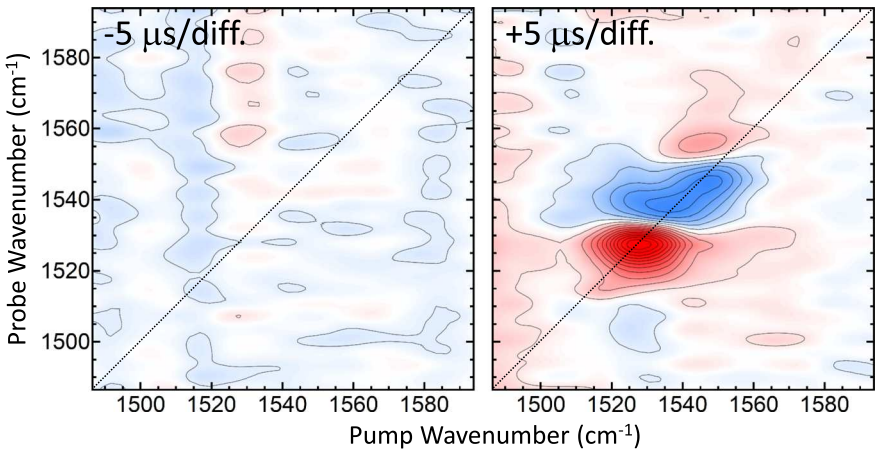

FIG. 3. Difference 2D IR spectra 5 μs before the actinic pump (left) and 5 μs after the actinic pump (right). The scale is magnified by a factor of 10 relative to that of Figs. 2(b) and 2(c).

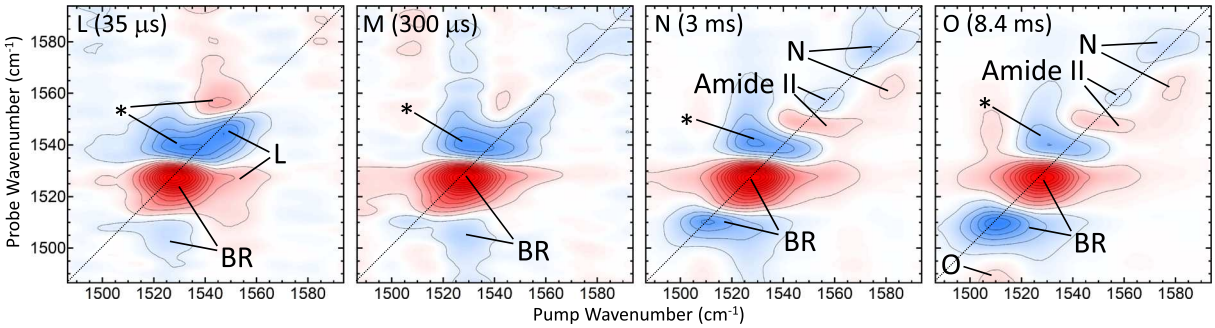

FIG. 4. Sequence of difference 2D IR spectra at delay times chosen to maximize the contributions from the L, M, N, and O intermediates. The scale is magnified by a factor of 10 relative to that of Figs. 2(b) and 2(c). Assignable spectroscopic features are labeled and discussed in the text.

band shifted to lower probe frequencies originating from its excited state absorption. Such a feature is indeed observed in all spectra (labeled BR in Fig. 4), albeit with varying intensities of the blue excited state absorption band, presumably due to partial cancellation effects.[22]

The L-intermediate exhibits a positive band at 1547 cm^{-1} in the transient 1D IR spectrum [Fig. 2(a)], very close to the bleach of the ethylenic stretch vibration. One can identify its 2D IR signature in the corresponding transient 2D IR spectrum at 35 μs (Fig. 4), which, however, strongly overlaps with the BR contribution. For the N-intermediate, the positive band is more separated at 1570 cm^{-1} [Fig. 2(a)] and correspondingly its transient 2D IR signature, which is labeled N in the 3 and 8.4 ms transient 2D IR spectra (Fig. 4). In either case, these are (positive) product bands; hence, the signs of their 2D IR peak pairs are not inverted, i.e., negative (blue) on the diagonal for the ground-state contribution and positive (red) for the anharmonically down-shifted excited state absorption.

There is another peak pair like that around 1555 cm^{-1}, labeled amide II in the 3 and 8.4 ms transient 2D IR spectra (Fig. 4). It has no obvious counterpart in the transient 1D IR spectrum [Fig. 2(a)], illustrating the resolution enhancement of 2D IR spectroscopy. The frequency coincides with the amide II band [Fig. 2(b)], indicating a response of the protein upon photo-switching.[44] The excited state contribution of the O-band at around 1510 cm^{-1} is visible in the 8.4 ms transient 2D IR spectrum as well. On the other hand, the assignment of the peaks labeled with an * in Fig. 4 is not clear at this point. Overall, the transient 2D IR spectra are surprisingly rich and call for an in-depth theoretical investigation.

V. CONCLUSION

In conclusion, a new application of 100 kHz Yb-laser systems has been introduced, transient 2D IR spectroscopy, using the photocycle of bacteriorhodopsin as a demonstration object. This approach utilizes the high repetition rate of these lasers in two ways: First, it directly determines the time resolution of the experiment (10 μs) and, at the same time, enables the measurement of many 2D IR spectra within a reasonable averaging time. Furthermore, the very good stability of the Yb-laser/OPA system allows for hours of measurement time without the need for any readjustments. We have not seen the same level of stability for Ti:S-based laser systems. Data can be taken overnight, and the only limiting aspect at this point is the need to refill the MCT detector with liquid N_2.

Currently, 100 kHz is the upper limit for this type of experiment, despite the fact that Yb-laser systems with higher repetition frequencies are available. The pulse shaper, the response time of the MCT detector, and the AD-converter limit the repetition frequency to that value.

The timescales covered by this type of experiment, 10 μs to a few tens of milliseconds, are perfectly suitable for the investigation of a wide range of photo-active proteins.[45] It also matches that of diffusion controlled bimolecular processes, such as protein–ligand interactions[46] or chemical reactions, in the context of artificial photosynthesis.[47] Even when the goal is "only" transient 1D IR spectroscopy [Fig. 2(a)], the system outperforms step-scan FTIR spectroscopy[40–42,44,48–50] or more modern setups based on quantum cascade lasers[51–54] in terms of measurement time; 1 min was sufficient to collect transient 1D IR data with the quality shown in Fig. 2(a). Admittedly, the present experimental setup is more expensive than, for example, a quantum cascade laser spectrometer, but not by orders of magnitudes (by a factor of 2–3). At the same time, due to the high intensities of femtosecond pulses, an Yb-laser system is much more versatile, as one may reach a very wide frequency range from THz[55] to x rays[1] by some means of nonlinear optics. The improvement over Ti:S lasers is enormous, suggesting that these types of lasers might become the standard for time-resolved mid-IR spectroscopy on all conceivable timescales, from femtoseconds to hours.

ACKNOWLEDGMENTS

The idea for this work was born after a discussion with Martin Zanni. Supply of the BR sample by Martin Engelhard (Max Planck Institute for Molecular Physiology), help from Olga Bozovic with the final sample preparation, and technical support and discussions from Jan Helbing are gratefully acknowledged. The work was supported by the Swiss National Science Foundation (SNF) through the NCCR MUST and under Grant No. 200020B_188694/1.

DATA AVAILABILITY

The data that support the findings of this study are openly available in Zenodo at http://doi.org/10.5281/zenodo.4557375.

REFERENCES

[1] D. O. Mücke, S. Alisauskas, J. A. Verhoef, A. Pugzlys, A. Baltuska, V. Smilgevicius, J. Pocius, L. Gininas, R. Danielius, and N. Forget, "Toward TW-peak-power single-cycle IR fields for attosecond physics and high-field science," in *Advances in Solid State Lasers Development and Applications* (IntechOpen, 2010), p. 297.

[2] Y. Zaouter, F. Guichard, L. Daniault, M. Hanna, F. Morin, C. Hönninger, E. Mottay, F. Druon, and P. Georges, Opt. Lett. **38**, 106 (2013).

[3] L. Lavenu, M. Natile, F. Guichard, Y. Zaouter, M. Hanna, E. Mottay, and P. Georges, Opt. Express **25**, 7530 (2017).

[4] S. B. Penwell, L. Whaley-Mayda, and A. Tokmakoff, Opt. Lett. **43**, 1363 (2018).

[5] C. R. Baiz, P. L. McRobbie, J. M. Anna, E. Geva, and K. J. Kubarych, Acc. Chem. Res. **42**, 1395 (2009).

[6] M. Khalil, N. Demirdöven, and A. Tokmakoff, J. Phys. Chem. A **107**, 5258 (2003).

[7] J. Zheng, K. Kwak, and M. D. Fayer, Acc. Chem. Res. **40**, 75 (2007).

[8] C. Minhaeng, *Two-Dimensional Optical Spectroscopy* (CRC Press, Boca Raton, 2009).

[9] P. Hamm and M. T. Zanni, *Concepts and Methods of 2D Infrared Spectroscopy* (Cambridge University Press, Cambridge, 2011).

[10] A. Ghosh, J. S. Ostrander, and M. T. Zanni, Chem. Rev. **117**, 10726 (2017).

[11] K. L. Koziol, P. J. M. Johnson, B. Stucki-Buchli, S. A. Waldauer, and P. Hamm, Curr. Opin. Struct. Biol. **34**, 1 (2015).

[12] B. M. Luther, K. M. Tracy, M. Gerrity, S. Brown, and A. T. Krummel, Opt. Express **24**, 4117 (2016).

[13] K. M. Tracy, M. V. Barich, C. L. Carver, B. M. Luther, and A. T. Krummel, J. Phys. Chem. Lett. **7**, 4865 (2016).

[14] G. Hithell, D. J. Shaw, P. M. Donaldson, G. M. Greetham, M. Towrie, G. A. Burley, A. W. Parker, and N. T. Hunt, J. Phys. Chem. B **120**, 4009 (2016).

[15] R. Fritzsch, P. M. Donaldson, G. M. Greetham, M. Towrie, A. W. Parker, M. J. Baker, and N. T. Hunt, Anal. Chem. **90**, 2732 (2018).

[16] P. M. Donaldson, G. M. Greetham, D. J. Shaw, A. W. Parker, and M. Towrie, J. Phys. Chem. A **122**, 780 (2018).

[17] K. M. Tracy, B. Guchhait, C. A. Tibbetts, B. M. Luther, and A. T. Krummel, ChemRxiv:9936464.

[18] S. Hume, G. M. Greetham, P. M. Donaldson, M. Towrie, A. W. Parker, M. J. Baker, and N. T. Hunt, Anal. Chem. **92**, 3463 (2020).

[19] K. M. Farrell, J. S. Ostrander, A. C. Jones, B. R. Yakami, S. S. Dicke, C. T. Middleton, P. Hamm, and M. T. Zanni, Opt. Express **28**, 33584 (2020).

[20] P. M. Donaldson, Chem. Sci. **11**, 8862 (2020).

[21] G. M. Greetham, P. M. Donaldson, C. Nation, I. V. Sazanovich, I. P. Clark, D. J. Shaw, A. W. Parker, and M. Towrie, Appl. Spectrosc. **70**, 645 (2016).

[22] J. Bredenbeck, J. Helbing, C. Renner, R. Behrendt, L. Moroder, J. Wachtveitl, and P. Hamm, J. Phys. Chem. B **107**, 8654 (2003).

[23] C. Kolano, J. Helbing, M. Kozinski, W. Sander, and P. Hamm, Nature **444**, 469 (2006).

[24] E. R. Andresen and P. Hamm, J. Phys. Chem. B **113**, 6520 (2009).

[25] B. Dereka, J. Helbing, and E. Vauthey, Angew. Chem., Int. Ed. **57**, 17014 (2018).

[26] J. Bredenbeck, J. Helbing, and P. Hamm, Rev. Sci. Instrum. **75**, 4462 (2004).

[27] X. Solinas, L. Antonucci, A. Bonvalet, and M. Joffre, Opt. Express **25**, 17811 (2017).

[28] K. C. Jones, C. S. Peng, and A. Tokmakoff, Proc. Natl. Acad. Sci. U. S. A. **110**, 2828 (2013).

[29] S.-H. Shim, D. B. Strasfeld, Y. L. Ling, and M. T. Zanni, Proc. Natl. Acad. Sci. U. S. A. **104**, 14197 (2007).

[30] C. T. Middleton, A. M. Woys, S. S. Mukherjee, and M. T. Zanni, Methods **52**, 12 (2010).

[31] S.-H. Shim, D. B. Strasfeld, E. C. Fulmer, and M. T. Zanni, Opt. Lett. **31**, 838 (2006).

[32] D. Oesterhelt and W. Stoeckenius, Nat., New Biol. **233**, 149 (1971).

[33] U. Haupts, J. Tittor, and D. Oesterhelt, Annu. Rev. Biophys. Biomol. Struct. **28**, 367 (1999).

[34] W. Kühlbrandt, Nature **406**, 569 (2000).

[35] A. H. Xie, J. F. Nagle, and R. H. Lozier, Biophys. J. **51**, 627 (1987).

[36] I. H. M. van Stokkum and R. H. Lozier, J. Phys. Chem. B **106**, 3477 (2002).

[37] J. Dobler, W. Zinth, W. Kaiser, and D. Oesterhelt, Chem. Phys. Lett. **144**, 215 (1988).

[38] Y. Feng, I. Vinogradov, and N.-H. Ge, Opt. Express **25**, 26262 (2017).

[39] D. Oesterhelt and W. Stoeckenius, Methods Enzymol. **31**, 667 (1974).

[40] C. Zscherp and J. Heberle, J. Phys. Chem. B **101**, 10542 (1997).

[41] K. Gerwert, Biol. Chem. **380**, 931 (1999).

[42] V. A. Lórenz-Fonfría and H. Kandori, Appl. Spectrosc. **61**, 428 (2007).

[43] S. O. Smith, M. S. Braiman, A. B. Myers, J. A. Pardoen, J. M. L. Courtin, C. Winkel, J. Lugtenburg, and R. A. Mathies, J. Am. Chem. Soc. **109**, 3108 (1987).

[44] K. Hauser, M. Engelhard, N. Friedman, M. Sheves, and F. Siebert, J. Phys. Chem. A **106**, 3553 (2002).

[45] T. Kottke, V. A. Lórenz-Fonfría, and J. Heberle, J. Phys. Chem. B **121**, 335 (2017).

[46] A. Bachmann, D. Wildemann, F. Praetorius, G. Fischer, and T. Kiefhaber, Proc. Natl. Acad. Sci. U. S. A. **108**, 3952 (2011).

[47] A. Rodenberg, M. Orazietti, B. Probst, C. Bachmann, R. Alberto, K. K. Baldridge, and P. Hamm, Inorg. Chem. **54**, 646 (2015).

[48] R. E. Murphy, F. H. Cook, and H. Sakai, J. Opt. Soc. Am. **65**, 600 (1975).

[49] W. Uhmann, A. Becker, C. Taran, and F. Siebert, Appl. Spectrosc. **45**, 390 (1991).

[50] I. Radu, M. Schleeger, C. Bolwien, and J. Heberle, Photochem. Photobiol. Sci. **8**, 1517 (2009).

[51] E. Ritter, L. Puskar, F. J. Bartl, E. F. Aziz, P. Hegemann, and U. Schade, Front. Mol. Biosci. **2**, 38 (2015).

[52] L. Zhang, G. Tian, J. Li, and B. Yu, Appl. Spectrosc. **68**, 1095 (2014).

[53] B.-J. Schultz, H. Mohrmann, V. A. Lorenz-Fonfria, and J. Heberle, Spectrochim. Acta, Part A **188**, 666 (2018).

[54] P. Stritt, M. Jawurek, and K. Hauser, Biomed. Spectrosc. Imaging **9**, 55 (2020).

[55] A. Shalit, S. J. Mousavi, and P. Hamm, J. Phys. Chem. B **125**, 581 (2021).